
Proceedings Paper:
Zaidi, SAR, Ghogho, M, McLernon, DC et al. (2014) Energy Harvesting Empowered Cognitive Metro-cellular Networks. In: Proceedings of the 1st International Workshop on Cognitive Cellular Systems. CCS 2014, 02-04 Sep 2014, Duisburg, Germany. Institute of Electrical and Electronics Engineers (IEEE). ISBN: 9781479941384.

https://doi.org/10.1109/CCS.2014.6933812

Energy Harvesting Empowered Cognitive Metro-cellular Networks

Syed Ali Raza Zaidi, *Student Member, IEEE,* Mounir Ghogho, *Senior Member, IEEE,* Desmond C. McLernon, *Member, IEEE,* and Ananthram Swami *Fellow, IEEE,*

Invited Paper

***Abstract*—Harvesting energy from natural (solar, wind, vibration etc.) and synthesized (microwave power transfer) sources is envisioned as a key enabler for realizing green wireless networks. Energy efficient scheduling is one of the prime objectives of cognitive radio platforms. To that end, in this article, we present a comprehensive analytical framework to characterize the performance of a cognitive metro-cellular network empowered by the solar energy harvesting. The proposed model considers both spatial and temporal dynamics of the energy field and the mobile user traffic. Channel uncertainties are also captured in terms of a large scale path-loss and a small-scale Rayleigh fading. A new metric called 'energy outage probability' which characterizes the self-sustainable operation of the base stations under energy harvesting is proposed and quantified. It is shown that the energy outage probability is strongly coupled with the path-loss exponent, required quality-of-service, base station and user density. Moreover, the energy outage probability varies both on a daily and yearly basis depending on the solar geoemtry. It is shown that even in winter time BS can run 10-15 hours without any purchase of energy from the power grid.**

***Index Terms*—energy harvesting, cognitive radio, metro-cells, solar irradiance, Hottell's model, Poisson point process, LTE, phantom cell**

I. Introduction

A. Motivation

THE term 'cognitive radio' is generally employed for an intelligent radio platform capable of exploiting transmission vacancies in an opportunistic manner. Nevertheless, the term cognition inherently possesses a broader meaning. Contrary to the common belief, cognition by no means is restricted to being an instrument for realization of the spectral gains. While spectral gains are necessary to mitigate the artificial spectrum scarcity, the future-proof radio design should also address network-wide energy efficiency. Notice that both the spectral efficiency and the energy efficiency are coupled together by the fact that both issues are exacerbated by the explosion in demand for any-time anywhere connectivity. Unfortunately, realizing green radios based on cognitive radio principles is not that straight-forward. This can be attributed to the fact that as compared to the traditional radios, the cognitive platform consume more power to gather the required intelligence about their operational environment. Moreover, the coexistence constraints enforced by the legacy network restrict the available degrees of freedoms too[1].

Harvesting energy from natural (solar, wind, vibration etc.) and synthesized (microwave power transfer) sources is envisioned as key enabler for realizing green wireless networks. In this context, cognitive radio based small cellular networks are envisioned to play a vital role. Thus definition of cognition must be extended and harvesting aware algorithms must be devised for the deployment of the self-sustainable networks. Energy harvesting and microwave power transfer have been extensively explored in context of cellular networks in [2], [3], [4], [5], [6], [7], [8] However, most of these studies assume the stochastic energy arrival models. In practice, energy harvested from the natural sources such as sun has a deterministic behavior. The only stochastic component is due to the environmental variations. Most of the stochastic models in literature are based on the probabilistic arrivals where energy arrival probability distributions are derived by averaging over the day times for several years. Consequently, these models cannot accurately predict energy deficiency of power at a given time or a day in a precise manner. Accurate prediction is of more interest to the cellular operator than an average performance metric. The average performance metric over a day ignores the variability of solar power over temporal dimension. Furthermore, most of these models only consider temporal dynamics of the energy arrival process. The spatial dimension of the arrival process is neglected by considering it to be identical and independent across various base stations. Nevertheless, in practice at a given time two base station in a spatial neighborhood experience similar amount of energy dispatch. More recently, Huang et al. [4] developed a spatial field model for energy harvesting. The model considers that the energy sources are distributed according to a Poisson point process in space and emit energy which decay according to the proposed power law. This model cannot be applied to natural energy harvesters such as solar panels because there is only a single source of energy (i.e., sun) the amount of energy available at a certain spatial location is function of solar irradiance and meteorological factors.

S. A. R. Zaidi, M. Ghogho and D. C. McLernon are with the School of Electronic and Electrical Engineering,University of Leeds, Leeds LS2 9JT, United Kingdom. E-mail: {elsarz,m.ghogho,d.c.mclernon}@leeds.ac.uk. M. Ghogho is also affiliated with the International University of Rabat, Morroco. Dr. Swami is affiliated with US Army Research Lab, Adelphi, U.S.A.

B. Contributions & Organization

In this paper, we present a comprehensive analytical model for the solar energy harvesting (Section II). We first present a mathematical characterization of the solar irradiance as the function of time and day number. We then utilize a well known solar irradiance model to characterize the maximum power which can be extracted from a photovoltaic (PV) solar panel. In section III, we formulate the spatio-temporal model for mobile users(MUs) and metro-cellular base stations (BSs). The metro-cellular networks are considered since small cell based densification by mounting platforms such as lightRadio™ on the lamp posts is becoming increasingly common. The lamp posts present an ideal opportunity for mounting both the solar panel and the metro-cells without any additional infrastructure deployment. Huawei has recently started to supply macro-cellular BSs with solar panels which are primarily targeted for the rural areas. Section IV, presents the outage probability analysis for metro-cellular networks. Based on the quality-of-service parameters such as desired downlink transmission rate and link reliability guarantees, we characterize the transmit power required to fulfill MUs demand. In Section VI, we employ the required transmit power to characterize the energy outage probability, i.e., the probability that a BS does not have sufficient energy to meet the downlink traffic demands. To the best of our knowledge, this is the first comprehensive study on the solar energy empowered cognitive metro-cellular networks.

II. Energy Harvesting: Modeling Solar Irradiance

In this section, we introduce and summarize key parameters which characterize the spatio-temporal behavior of the solar power field. The key measure of the rate at which the solar power arrives on a unit area over the earth's surface is termed as 'solar irradiance'. Solar irradiance is the radiative flux and thus measured in W/m^2.

A. Extra-terrestrial Solar Irradiance

Solar irradiance is an instantaneous measure of the energy arrival rate and thus varies across both the spatial and the temporal domain. Quantification of solar irradiance requires a comprehensive description of the underlying meteorological parameters. To this end, in this subsection, we provide an overview of these parameters and detail their interrelationship.

The radiation intensity at sun's surface is $6.33\times10^7\,W/m^2$. Earth revolves around sun in an elliptical orbit. The mean separation between earth and sun is $r_{SE} = 1.496\times10^8\,km$ (also known as $1\,AU$ astronomical unit). Due to the distance squared spread of the radiant power the amount of solar energy received outside earths atmosphere is reduced to $I_{SCon} = 1367\,W/m^2$. The constant I_{SCon} is frequently refered to as the 'solar constant'. The irradiance measured outside earth's atmosphere is generally termed as the extra-terrestrial (ET) solar irradiance. The ET solar irradiance varies by $\pm3.4\%$ due to variation in the distance between the sun and the earth. The maxima occurs in January (perihelion) while the minima occurs in July (aphelion) [9], [10]. Mathematically, this variation can be accommodated in the definition of the solar irradiance as

$$\bar{I}_{ET} = I_{SCon}\left[1+0.034\cos\left(\frac{360N}{365.25}\right)\right]\,W/m^2, \tag{1}$$

where $N\in\{1,...,365\}$ is the day number. Moreover, the irradiance falling on the a flat surface located on the earth experience a so called 'cosine effect'. The cosine effect dictates that $\bar{I}_{ET}$ is reduced by a factor $\cos(\theta_z)$ where θ_z is the angle between the plane located on the earth's surface and its rotation which is normal to the sun's rays. The ET irradiance is then quantified as

$$I_{ET} = \bar{I}_{ET}\cos\theta_z, \tag{2}$$

The angle θ_z is more frequently known as the 'solar zenith angle' and is function of both the time and the spatial location of PV module. Specifically, the zenith angle can be expressed as

$$\cos\left(\theta_z\left(t\right)\right) = \sin\delta\sin\omega + \cos\omega\cos\delta\cos h\left(t\right), \tag{3}$$

where, δ is the earth's declination angle; ω is the latitude and $h(t)$ is the hour angle. The declination angle is defined as the angle made between a ray of the sun extended to the center of the earth and the equitorial plane. Declination angle suffers daily change of maximum 0.5° and can be mathematically evaluated as [10]

$$\delta = 23.45^\circ\times\sin\left(\frac{360(284+N)}{365.35}\right). \tag{4}$$

A more accurate model was given by Spencer [11] with maximum error of 0.05°

$$\begin{aligned}\delta &= 0.006918 - 0.399912\cos\left(\Upsilon\right) + 0.070257\sin\left(\Upsilon\right)\\ &- 0.006758\cos\left(2\Upsilon\right) + 0.000907\sin\left(2\Upsilon\right)\\ &- 0.002697\cos\left(3\Upsilon\right) + 0.00148\sin\left(3\Upsilon\right)\\ &\text{with}\,\Upsilon = \frac{2\pi\left(N-1\right)}{365}.\end{aligned} \tag{5}$$

The term $h(t)$ in (3) refers to the hour angle which can be quantified from the concept of the solar day and equation of time. A solar day in general corresponds to the time elapsed between to consecutive crossings of the sun. It has the mean duration of 24 hrs with variation of up to 30s . These variations occur due to elliptical path of the earth around sun and tilt of earth with respect to its axis. The offset between the local standard time and the sun standard time can be determined as

$$T_{off} = E_t - 4\times\text{Longitude} + 60\times\text{time zone}, \tag{6}$$

where E_t is the equation of time (see [9]for details). The hour angle is then given by

$$TST = \text{Hours}\times60 + \text{Minutes} + \frac{\text{Seconds}}{60} + T_{off}, \tag{7}$$

$$h(t) = \frac{TST}{4} - 180. \tag{8}$$

Numerous analytical models have been formulated from Eq.(2) to characterize the solar energy received by a PV module under clear-day conditions [12]. These models account for both the direct and diffuse components of solar irradiance on the PV module. In this article, we employ a simple yet accurate Hottell's clear day model [10] to characterize the global horizontal irradiance (i.e., amount of power received at a typical PV module). Consequently, solar radiation at time t is given by

$$I_H = \overbrace{\bar{I}_{ET}\cos\theta_z(t)\left[\kappa_1-\kappa_2\left(a_o+a_1\exp\left(-k\sec\theta_z\left(t\right)\right)\right)\right]}^{\text{Diffuse component}} \tag{9}$$

$$+ \underbrace{\bar{I}_{ET}\left[a_o+a_1\exp\left(-k\sec\theta_z\left(t\right)\right)\right]}_{\text{Direct component}}, \tag{10}$$

where $\kappa_1 = 0.2710$, $\kappa_2 = 0.2939$ and for urban 5-km visibility haze model the remaining parameters are

$$\begin{aligned}a_o &= 0.2538 - 0.0063\left(6-H\right)^2,\\ a_1 &= 0.7678 + 0.0010\left(6.5-H\right)^2,\\ k &= 0.249 + 0.081(2.5-H)^2,\end{aligned} \tag{11}$$

with H being the local elevation in kilometers. For the cellular BSs, $H = H_e + H_b$ where H_e is the elevation of the terrain and H_b is the BS height.

B. Cloud cover and Atmosphere

The global horizontal irradiance is severely effected by the cloud cover, atmospheric scattering and absorption. In Hottell's model the parameter k is the measure of sky-clearness. The sky clearness is generally described in terms of clearness index which varies between 0 and 1. Several authors have studied the distribution of clearness index to quantify the impact of atmospheric conditions. In this article, we restrict our discussion to the urban haze clearity model of Hottell [10]. Notice that the cloud cover and atmospheric scattering can be included by a straight-forward scaling. The key objective of this article is to explore the design space of cognitive cellular networks under energy harvesting phenomenon. Thus we restrict the parameter space to realistic size so that performance guarantees can be obtained without any loss of generality.

C. Modeling PV Panel & Output Power

The global horizontal irradiance is converted in to an effective output power by employing PV panels. More specifically, the output power of the PV module is the function of both the time of the day and the spatial location of the panel through the irradiance.

In this article, we adapt a simple single diode based circuit model of a solar cell which was proposed in [13]. The current at the output of the PV module can then be expressed as

$$I_{PV} = I_{sc}\left[1-\kappa_3\left\{\exp\left(\frac{V_{PV}}{\kappa_4 V_{oc}}\right)-1\right\}\right], \tag{12}$$

where $\kappa_3 = \left(1-\frac{I_{MPP}}{I_{sc}}\right)\exp\left(\frac{V_{MPP}}{\kappa_4 V_{oc}}\right)$ and $\kappa_4 = \left(\frac{V_{MPP}}{V_{oc}}-1\right)/\ln\left(1-\frac{I_{MPP}}{I_{sc}}\right)$ which depends on the module parameters: (i) short circuit current I_{sc}; (ii) open circuit voltage V_{oc}; (iii) maximum power point voltage V_{MPP} and (iv) maximum power point current I_{MPP}. These parameters can be expressed as the function of ambient temperature and global horizontal irradiance as

$$I_{sc} = I_{scs}\times\frac{I_H}{I_S}\times\left[1+\varsigma_1(T-T_s)\right], \tag{13}$$

$$V_{oc} = V_{ocs} + \varsigma_2(T-T_s), \tag{14}$$

$$I_{MPP} = I_{MPPS}\times\frac{I_H}{I_S}\times\left[1+\varsigma_1(T-T_s)\right], \tag{15}$$

$$V_{MPP} = V_{MPPS} + \varsigma_2(T-T_s), \tag{16}$$

where I_{scs}, V_{ocs}, I_{MPPS},V_{MPPS} are defined at standard conditions, i.e., $I_S = 1000\,W/m^2$ and $T_s = 25^\circ C$ with$\varsigma_1$and ς_2 being the current and the voltage coefficient. These parameters are generally provided in the data sheet of a PV module. For the purpose of this

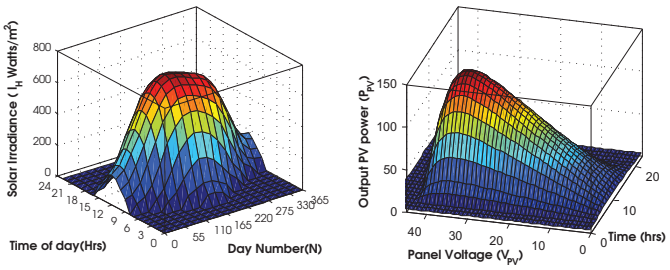

(a) Global Horizontal Irradiance by Hottell's model for Nottingham with LAT= 52.95, LONG=1.1333 and Elevation $H = H_e + H_b = 117 + 6$ (see Eq. (9)).

(b) Maximum Output power of PV panel vs. Voltage and time of day in hrs with $N = 162$, i.e., 12^{th} July and $T = 25^oC$ (see Eq. (12)).

Figure 1. Global Horizontal Irradiance and PV output power.

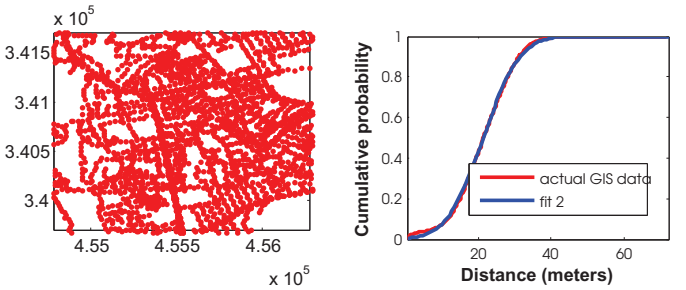

(a) Snapshot of a point pattern formed by Lamp posts in Nottingham City.

(b) Nearest Neighbor Distance Distribution for Poisson point process vs. the Measured Data, i.e., $\lambda_{LP} = 0.48 \times 10^{-3}$.

Figure 2. HPPP based modeling of lamp posts in Nottingham city.

study, the numerical values of these parameters are borrowed from the data sheet of PW1650-24V as in [13].

From Eq. (12), the output power of the PV panel can be computed as the function of voltage as $P_{PV} = I_{PV}V_{PV}$. Most of the modern day panels are equipped with the maximum power point tracking algorithms [1]. The maximum output power can be extracted by adjusting the cell load resistance. The maximum extracted power is denoted by P_{PV}^{max} and is computed by maximizing P_{PV} with respect to output voltage. Fig. 1 graphically illustrate variations of the global horizontal irradiance and maximum output power of the PV panel.

III. Spatio-temporal Modeling of MUs & Metro cells

In the previous section, we introduced the solar energy harvesting model. It was shown that the amount of power harvested by a panel possesses both spatial and temporal variations. In the context of cellular networks, the number of MUs in each cell also exercises spatio-temporal dynamics. To this end, objective of this section is to present model for active MUs in the downlink of a metro cell.

A. Network Architecture

In this article, we consider a metro-cellular network operating in the presence of macro tier. Similar to the phantom small cellular architecture proposed by DOCOMO in [14], [15], metro-cells are deployed in a non co-channel mode. Specifically, both the metro and the macro cells operate on the different frequency bands. The architecture leverages the master-slave relationship between the macro and the metro cells to provide a robust and a scalable solution for the rapid deployment of high throughput small cells. Small cells are delegated the responsibility of serving throughput intensive MUs while macro-cell is responsible for handling the signaling and association. The architecture result in control and capacity plane separation (frequently known as C/U plain split) providing support for adding capacity on-demand.

Spatial Model for Metro-cells

It is envisioned that the metro-cell deployment will exploit existing infrastructure such as street lamp posts. The lamp posts are ideal spot for mounting the solar panels too. Lamp posts are generally connected to the power grid and hence in the absence of sufficient power from the energy harvester, power can be drawn from the grid. It is also possible to devise a street level junction box where the output of solar panel can be fed to an inverter or a storage device such as battery. These junction boxes can then employ intelligent prediction and forecasting algorithms to minimize the operational expense (OPEX) by maximizing the use of harvested power. In this paper, we assume that metro-cells are deployed on the lamp posts.

In recent past, stochastic geometry has been used extensively for analyzing the performance of the large scale cellular and ad hoc cognitive networks [16], [17]. Most of the studies, assume that the spatial distribution of the BSs follow a Homogeneous Poisson point process (HPPP). The key advantage of employing the HPPP based models is analytical tractability of performance metrics such as coverage and ergodic rate. For the metro-cellular networks, it is not obvious whether the spatial distribution of lamp posts can be modeled as a HPPP. To this end, we considered the actual geographical data for the lamp posts in Nottingham city [18]. Fig. 2-a depicts the Point pattern of the actual lamp posts. From the snapshot it is obvious that while lamp post exercise some degree of repulsion and regularity, there is still sufficient randomness in location, embedded due to the urban geometry. More specifically, while the street lamps inside a street may look uniformly spaced, on the neighborhood scale they form a random point pattern. This is due to the variability in street directions, street widths, lamp post deployment patterns, availability of power supply etc.

This motivates us to test the spatial point pattern formed by the lamp posts using nearest neighbor statistics for complete spatial randomness. We applied Clark-Evans test for the cumulative distribution function (CDF) of nearest neighbor distances of the lamp post. As stated by the test criterion, the distribution should converge to Gaussian probability law with a mean $1/2\sqrt{\lambda}$ and a variance $\frac{4-\pi}{4\lambda\pi}$. We verified the mean, variance and the distribution itself by using distribution fitting tool in MATLAB. The CDF of the measured nearest neighbor distance distribution and the one obtained under the Poisson hypothesis are depicted in Fig. 2-b .

In brief, for the rest of the discussion, we assume that the spatial configuration of the metro-cellular network is captured by a HPPP Π_M with intensity λ_M. More specifically, the probability of finding $n \in \mathbb{N}$ metro BSs inside a region $\mathcal{A} \subseteq \mathbb{R}^2$ is given by

$$\mathbb{P}\left(\Pi_M(\mathcal{A}) = n\right) = \frac{\left(\lambda_M v_2(\mathcal{A})\right)^n}{n!} \exp\left(-\lambda_M v_2(\mathcal{A})\right), \qquad (17)$$

where, $v_2(\mathcal{A}) = \int_{\mathcal{A}} \boldsymbol{dx}$ is the Lebesgue measure on $\mathbb{R}^2$[**?**] and $\lambda_M = \rho_{LS}\lambda_{LP}$ is the average number of metro-cell BSs per unit area as a function of the lamp post density λ_{LP}. If $\mathcal{A}$ is a disc of radius r then $v_2(\mathcal{A}) = \pi r^2$. Notice, that a point processΠ_M can also be considered as a counting measure. Furthermore, we consider that only a fraction of the lamp posts can be rented from the city council for the deployment of the metro cells. Consequently, ρ_{LS} is the fraction which is function of the operators OPEX.

B. Spatio Temporal Model for MUs

We assume downlink operation of the metro-cells where MUs average density in each metro-cell varies as [19]

$$\lambda_U(t) = \lambda_U \underbrace{\left(\kappa_5 - \kappa_6 \sin\left(2\pi \frac{(t-\phi)}{24}\right)\right)}_{U(t)}, \qquad (18)$$

such that κ_5 and κ_6 are traffic related constants which lie in interval $[0, 1]$ so that $|U(t)| = 1$. These parameters depend on the type of

[1] sometimes implemented at inverter level rather than panel level

the day, i.e., weekend or weekday etc. The sinusoidal variation of mean density has been derived from actual cellular network in [19] and [20]. In this study, we assume operation on a typical weekday by selecting the values of$\kappa_5 = \kappa_6 = 0.5$ and $\phi = -1$. These parameters produce well known characteristic of the user arrival such as decreasing behavior for early hours, dip at around 4-5 a.m and maxima around the evening time.

The spatial distribution of users is captured using a HPPP Π_U with mean $\lambda_U(t)$ at an arbitrary time instant t, this follows from the observations made in [20]. In [20] authors, demonstrated that the active downlink users are distributed according to PPP. Since the active users at a certain time in a cell are also the number of users distributed across space, the HPPP based modeling of MUs is a quite reasonable assumption. MUs are served by the metro-cells which are nearest to the MU. In other words, the MUs are served by a corresponding metro-cell whose voronoi region contains MU.

C. Channel Model and Scheduling

In this study, we assume that the downlink operation of the metro-cells is noise-limited. The co-channel interference between the metro-cells is negligible. In practice, a LTE resource grid is comprised of say $K = 12$ sub-channels and $M = 10$ sub-frames each corresponding to 1 transmit time interval (TTI). Leveraging the master-slave relationship the macro-cell can schedule metros such that a spatial neighborhood of K cells transmit on different sub-channels. Each metro-cells then employs M sub-frames to schedule its user by employing either a channel aware or a channel blind scheduling strategy. Consequently, interference from say the K^{th} metro-cell to the MU is negligible.

We assume that the communication between an arbitrary metro-cell and its scheduled MU suffers from a Rayleigh block-fading environment. The overall channel gain between a transmitter and a receiver separated by distance R is modeled as $Hl(R)$. Here, H is a unit mean Exponential random variable and $l(R) = C(1+R^{\alpha})^{-1}$ is the power-law path-loss function. The path-loss function depends on the distance R, a frequency dependent constant C and an environment/terrain dependent path-loss exponent α. The fading channel gains are assumed to be mutually independent and identically distributed (i.i.d.) across different links. Without any loss of generality, we will assume $C = 1$ for the rest of this discussion.

IV. Quality-of-Service & Transmit Power Selection

The aim of this section is to quantify the transmit power required to serve an MU such that its Quality-of-Service (QoS) requirements are satisfied. The QoS constraint is expressed in terms of desired rate and the link reliability constraint as follows:

$$\mathbb{P}_{out}^{MU} = \Pr\left\{f\left(\text{SNR}\right) < R_o\right\} \leq 1 - \rho_{th}, \tag{19}$$

here R_o is the MU's desired downlink rate and ρ_{th} is the link reliability constraint. Notice that the instantaneous attainable rate C is expressed as the function of signal-to-noise ratio (SNR) as $f(SNR)$. The key motivation is to maintain the generality in analysis so that either Shannon capacity type formulation for LTE as in [21] or the arctangent based saturated throughput function as in [22] both can be adopted for quantification of the transmit power. The advantage of the later over the former is that it also allows investigation of adaptive modulation and coding schemes. For the sake of this exposition, we restrict our discussion to $f(\text{SNR}) = \log_2\left(1 + \text{SNR}\right)$.

Theorem 1. *The transmit power P_{MC} which a metro-cell must adapt in order to satisfy the MU's desired QoS constraint expressed in Eq. (19) can be expressed as the function of the path-loss exponent, base station density and reliability constraint as follows*

$$P_{MC} \geq \frac{f^{-1}\left(R_o\right)\sigma^2}{\ln\left(\rho_{th}^{-1}\right)}\left[1 + \frac{\Gamma(1+1/\delta)}{\left(\lambda_M \pi\right)^{\delta}}\right], \tag{20}$$

where $\Gamma(a) = \int_0^{\infty} x^{a-1}\exp(-x)dx$ is the Gamma function , σ^2 is noise variance and $\delta = 2/\alpha$.

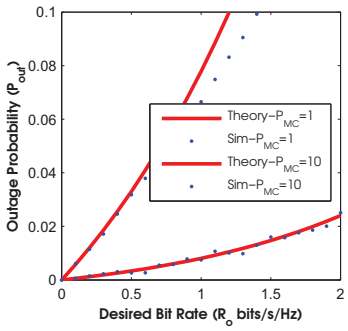

Figure 3. Outage probability of MU vs. desired bit rate R_o in bits/s/Hz for varying values of P_{MC} with $\sigma^2 = -70\,dB/Hz$, $\lambda_{LP} = 0.48 \times 10^{-3}$, $\rho_{LS} = 0.3$ and $\alpha = 4$ (see Eq. (20)).

Proof: The outage probability of an arbitrary MU can be evaluated as

$$\begin{aligned}
\mathbb{P}_{out}^{MU} &= 1 - \Pr\left\{SNR > f^{-1}(R_o)\right\} \\
&= 1 - \Pr\left\{\frac{P_{MC}Hl(R)}{\sigma^2} > f^{-1}(R_o)\right\} \\
&\overset{(a)}{=} 1 - \mathbb{E}_Z\left[\exp\left(-\frac{f^{-1}(R_o)\sigma^2}{P_{MC}z}\right)\right], \\
&= 1 - \exp\left(-s\right)\mathbb{E}_Z\left[\exp\left(-sz\right)\right] \\
&= 1 - \exp\left(-s\right)\mathcal{L}_Z(s)|_{s=\frac{f^{-1}(R_o)\sigma^2}{P_{MC}z}}.
\end{aligned} \tag{21}$$

where (a) follows from the fact that H is exponential random variable with unit mean. The term $\mathcal{L}_Z(s)$ corresponds to the Laplace transform of random variable $Z = R^{\alpha}$. Since, MUs are served by the closest metro-cells the distribution of Z can be determined from the nearest neighbor distribution of the HPPP as

$$f_Z\left(z\right) = \lambda_M \pi \delta z^{\delta-1}\exp\left(-\lambda_M \pi z^{\delta}\right). \tag{22}$$

Notice that Z follows Weibull distribution whose Laplace transform cannot be expressed in closed form. Consequently, we exploit the concavity of the Laplace transform $\mathbb{E}_Z\left[\exp\left(-sz\right)\right] \leq \exp\left(-s\mathbb{E}_Z(z)\right)$ by applying Jensen's inequality to obtain upper bound on outage probability of the MU. The bounds obtained are verified with the help of Monte-Carlo Simulations as shown in Fig. 3. For the region of interest, i.e., $1 - \rho_{th} \leq 0.1$ the proposed bound is reasonably tight thus outage probability of MU can be expressed in closed form as

$$\mathbb{P}_{out}^{MU} = 1 - \exp\left(-\frac{f^{-1}(R_o)\sigma^2}{P_{MC}}\left(1 + \frac{\Gamma(1+1/\delta)}{\left(\lambda_M\pi\right)^{\delta}}\right)\right). \tag{23}$$

Inverting the expression by enforcing the reliability constraint concludes the proof. ∎

V. Energy Outage Probability

The energy outage probability of the metro-cellular network is defined as

$$\mathbb{P}_{out}^{E} = \Pr\left\{N_u\left(t\right)P_{MC} > P_{PV}^{max}\right\}, \tag{24}$$

where P_{PV}^{max} is the maximum harvested power at time instant t as defined in Section II and $N_U(t)$ is the number of active downlink users in an arbitrary metro-cell. Notice that for the sake of tractability, we do not consider energy storage model. We assume that the harvested energy can be utilized on a sub-hourly basis to schedule transmissions. In the event of energy outage, the deficit is purchased from the power grid. A more practical system would utilize energy storage such as Lithium Ion batteries to maximize the energy utility by harvesting in early hours of day when traffic is low and spending it later in the evenings.

Theorem 2. *The energy outage probability of the metro-cellular network which schedules its MUs by considering their desired rate*

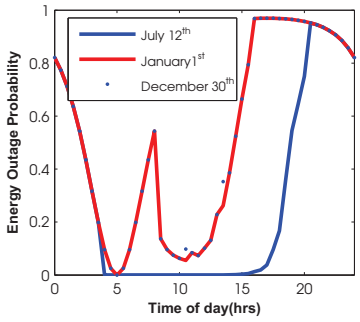

Figure 4. Energy outage probability of metro-cellular network for $\lambda_U = 6 \times \lambda_M$, $\rho_{th} = 0.9$, $\alpha = 4$, $\lambda_{LP} = 0.48 \times 10^{-3}$, $\rho_{LS} = 0.3$ and $\sigma^2 = -70\,dB/Hz$ (see Eq.(25)).

R_o and reliability threshold ρ_{th} is function of the number of active users, the day number (i.e., time of the year), the time of the day, density of base stations (through P_{MC}) and the propagation conditions. It can be characterized as

$$\mathbb{P}^E_{out} = 1 - \sum_{i=0}^{\lceil P^{max}_{PV}/P_{MC} \rceil} \frac{\kappa_7^{\kappa_7+1}\Gamma\left(i+\kappa_7+1\right)\left(\lambda_U(t)/\lambda_M\right)^i}{i!\Gamma\left(\kappa_7+1\right)\left(\lambda_U(t)/\lambda_M+\kappa_7\right)^{i+\kappa_7+1}}, \tag{25}$$

where $\kappa_7 = 3.5$ is the constant and $\lceil x \rceil$ denotes nearest integer to x.

Proof: Details omitted due to lack of space, the derivation follows from the Gamma distribution of the area of voronoi cell and the Poisson distribution of MUs at time t. ■

Discussion

Fig. 4 depicts the energy outage probability of the solar empowered metro cells against varying time of the day for various days in a year. It can be observed that for the summer time (July 12^{th}) the harvested energy is significantly higher than the winter time (January/December). Thus as expected the energy outages are more likely during winters. Nevertheless, even during winter around 10 hours of operation can be guaranteed by instantaneous expenditure of harvested solar power. With practical solar energy storage systems the performance can be improved significantly as the surplus energy during afternoons can be used in the evenings. The energy outage probability is also couple with λ_U. More specifically it decreases with an increase in mean number of peak hour user per cell. In this paper, we considered $\lambda_U = \lambda_M N_s$ where $N_s = 6$ was used so that the maximum number of user in a voronoi cells does not exceed the numerical value of 10, i.e., each metro-cell which is mounted on the lamp post serves around 6-10 users in peak hours.

VI. Conclusion & Future work

In this paper, we presented a comprehensive analytical framework to investigate the performance of a solar empowered metro-cellular network. We departed from the traditional definition of cognition which focuses on the spectral efficiency performance and characterized cognition in terms of energy efficiency. It is shown that both temporal and spatial dynamics of solar energy field and mobile user traffic are critical in shaping the network-wide energy requirement. The energy demand of a metro-cellular BS is also strongly coupled with the quality-of-service desired by MUs. In this paper, we focused on a homogenous mobile user case where demands are similar. However, the model proposed in the paper can be extended for heterogeneous user demands. It is expected that under heterogeneous demands the harvesting energy can further reduce the operational expenses by reducing needs for purchasing power from grid suppliers. It is shown that a metro-cellular network is self sustainable in terms of energy for around 10-15 hours of a day depending on the time of the year. In future, we plan to extend the framework to devise harvesting aware scheduling algorithms which balance the tradeoffs between throughput and energy consumption of the network to realize truly green cognitive cellular networks.

References

[1] S. Raza Zaidi, M. Ghogho, and D. McLernon, "Breaking area spectral efficiency wall in cognitive underlay networks," November 2014.

[2] K. Huang and V. Lau, "Enabling wireless power transfer in cellular networks: architecture, modeling and deployment," 2012.

[3] K. Huang and E. G. Larsson, "Simultaneous information and power transfer for broadband wireless systems," 2012.

[4] K. Huang and V. O. Li, "Renewables powered cellular networks: Energy field and network coverage," *arXiv preprint arXiv:1404.2074*, 2014.

[5] Y. Guo, J. Xu, L. Duan, and R. Zhang, "Joint energy and spectrum cooperation for cellular communication systems," *arXiv preprint arXiv:1312.1756*, 2013.

[6] S. Lee, R. Zhang, and K. Huang, "Opportunistic wireless energy harvesting in cognitive radio networks," 2013.

[7] G. Yang, C. K. Ho, R. Zhang, and Y. L. Guan, "Throughput optimization for massive mimo systems powered by wireless energy transfer," *arXiv preprint arXiv:1403.3991*, 2014.

[8] H. Wang, H. Li, Z. Wang, X. Chen, and S. Ci, "Stochastic queue modeling and key design metrics analysis for solar energy powered cellular networks," in *Computing, Networking and Communications (ICNC), 2014 International Conference on*. IEEE, 2014, pp. 472–477.

[9] D. Heinemann, *Energy Meteorlogy*. Oldenburg, 2002, vol. 1.

[10] W. B. Stine and M. Geyer, *Power from the Sun*. Power from the sun. net, 2001.

[11] J. Spencer, "Fourier series representation of the position of the sun," *Search*, vol. 2, no. 5, p. 172, 1971.

[12] C. A. Gueymard, "Direct solar transmittance and irradiance predictions with broadband models. part i: detailed theoretical performance assessment," *Solar Energy*, vol. 74, no. 5, pp. 355–379, 2003.

[13] A. Bellini, S. Bifaretti, V. Iacovone, and C. Cornaro, "Simplified model of a photovoltaic module," in *Applied Electronics, 2009. AE 2009*. IEEE, 2009, pp. 47–51.

[14] H. Ishii, Y. Kishiyama, and H. Takahashi, "A novel architecture for lte-b: C-plane/u-plane split and phantom cell concept," in *Globecom Workshops (GC Wkshps), 2012 IEEE*. IEEE, 2012, pp. 624–630.

[15] S. Mukherjee and H. Ishii, "Energy efficiency in the phantom cell enhanced local area architecture," in *Wireless Communications and Networking Conference (WCNC), 2013 IEEE*. IEEE, 2013, pp. 1267–1272.

[16] J. G. Andrews, F. Baccelli, and R. K. Ganti, "A tractable approach to coverage and rate in cellular networks," *Communications, IEEE Transactions on*, vol. 59, no. 11, pp. 3122–3134, 2011.

[17] S. Zaidi, M. Ghogho, D. Mclernon, and A. Swami, "Achievable spatial throughput in multi-antenna cognitive underlay networks with multi-hop relaying," *Selected Areas in Communications, IEEE Journal on*, vol. 31, no. 8, pp. 1543–1558, August 2013.

[18] Nottingham. (214, Jul) Open data nottingham: Street lights. [Online]. Available: http://www.opendatanottingham.org.uk/dataset.aspx?id=35

[19] E. Oh and B. Krishnamachari, "Energy savings through dynamic base station switching in cellular wireless access networks," in *Global Telecommunications Conference (GLOBECOM 2010), 2010 IEEE*. IEEE, 2010, pp. 1–5.

[20] M. Laner, P. Svoboda, S. Schwarz, and M. Rupp, "Users in cells: a data traffic analysis," in *Wireless Communications and Networking Conference (WCNC), 2012 IEEE*. IEEE, 2012, pp. 3063–3068.

[21] P. Mogensen, W. Na, I. Z. Kovács, F. Frederiksen, A. Pokhariyal, K. I. Pedersen, T. Kolding, K. Hugl, and M. Kuusela, "Lte capacity compared to the shannon bound," in *Vehicular Technology Conference, 2007. VTC2007-Spring. IEEE 65th*. IEEE, 2007, pp. 1234–1238.

[22] W. Guo, S. Wang, and X. Chu, "Capacity expression and power allocation for arbitrary modulation and coding rates," in *Wireless Communications and Networking Conference (WCNC), 2013 IEEE*. IEEE, 2013, pp. 3294–3299.